Hindawi
Mathematical Problems in Engineering
Volume 2020, Article ID 3821591, 15 pages
https://doi.org/10.1155/2020/3821591

*Research Article*

# Comparative Analysis of Optimization Models for Paired Intersections with Left-Turn Bays

**Ronghan Yao, Wensong Zhang, and Meng Long**

*School of Transportation and Logistics, Dalian University of Technology, Experimental Building No. 4, Linggong Road No. 2, Ganjingzi District, 116024 Dalian, China*

Correspondence should be addressed to Ronghan Yao; cyanyrh@dlut.edu.cn

Received 18 October 2019; Revised 26 December 2019; Accepted 7 January 2020; Published 10 February 2020

Academic Editor: Libor Pekař



Left-turn bays may be provided at paired intersections when heavy left-turn demands exist on some approaches. Such left-turn bays may have significant effects on intersection operations. Considering the settings of left-turn bays, two single-objective optimization models are developed for paired intersections with uncoordinated and coordinated signals, respectively. Numerical examples are fulfilled to demonstrate and compare the formulated models, and the orthogonal simulation experiments are carried out. Assuming that the relevance of traffic flow exists, the results show that the optimized effective green times and left-turn bay lengths depend on traffic demand, whereas the optimized offset between paired intersections is sensitive to intersection spacing; the optimization model with coordinated signals outstrips that with uncoordinated signals at 99% confidence level when the distance between paired intersections is not too far and traffic demand is not too low, whereas the former may be inferior to the latter when traffic demand is low enough and intersection spacing is far enough.

## 1. Introduction

To accommodate the relatively heavy left turns at intersections, left-turn bays (i.e., short left-turn lanes) are usually provided on intersection approaches so that the capacity and level of service of the entire intersection can be improved. The length of such a left-turn bay is generally limited, but such turn bays (i.e., short lanes) are viewed as normal exclusive turn lanes in the Highway Capacity Manual [1]. Such a treatment ignores the impacts of turn bays on traffic flow operations because of being underused.

In the recent decades, many researchers discussed the effects of turn bays on capacity, delay, and number of stops. Messer and Fambro [2] investigated the effects of signal phasing and left-turn bay length on left-turn capacity and gave the mathematical relationships between reductions in left-turn capacity and geometric and traffic conditions. Akçelik [3] denoted that the saturation flow rate might not be a constant for the lane group with a turn bay and put forward the calculation formula for the average saturation flow rate for such a lane group. Lee et al. [4] proposed the models to predict lane utilization factors for six intersection types and to assess the effects of low lane utilization on intersection capacity and level of service. Sando and Moses [5] analyzed the influences of many geometric factors on the operation of triple left-turn lanes with or without turn bays. Tian and Wu [6] developed a capacity estimation model for a signalized intersection with a short right-turn lane. Wu [7] presented a theoretical-empirical model to estimate the total approach capacity at signalized intersections with short left-turn lanes and shared through-right lanes. Zhang and Tong [8] used a probabilistic approach to model the capacity of the left-turn and through movements as a function of the left-turn bay length. Osei-Asamoah et al. [9] determined the important factors of left-turn lane spillover and modelled the expected through movement capacity and discharge rate. Also, the theoretical delay models were given for protected left-turn operations at signalized intersections with left-turn bays during heavy traffic [10]. Li and Elefteriadou [11] proposed a method to maximize the throughput of an approach with left-turn or

right-turn bays and suggested to repeat the phase twice in the cycle for such an approach.

On the contrary, some scholars investigated the determination of the required turn bay length. Kikuchi et al. [12] analyzed the probability of overflow or blockage of a left-turn bay and proposed the models to provide the required length of a left-turn bay for different traffic conditions. They also discussed the determination of the left-turn bay length under different cases, such as double or dual left-turn bays [13], three-branch fork lanes (left-turn, through, and right-turn lanes) from a single lane [14], and a left-turn bay under different left-turn signal schemes [15]. Qi et al. [16] described a procedure to estimate the queue storage length, deceleration length, and total design length of a left-turn bay in peak and off-peak hours. Yang and Zhou [17] denoted that determining the design length of left-turn lanes by the sum of queue storage length and deceleration length was appropriate at unsignalized intersections but inapplicable to signalized intersections and proposed a methodology that coordinated the requirement of each component with signal timings for the proper design of left-turn lanes.

For signalized intersections, the effective green time per phase is a decision variable to represent the allocation of temporal resources, while the length of each left-turn bay is a decision variable to represent the allocation of spatial resources [18–20]. The abovementioned research only focused on left-turn bays at isolated intersections. Actually, left-turn bays are sometimes provided at paired intersections, especially, on the common road section. For this case, the optimal allocation of temporal-spatial resources is worth being studied. While the distance between paired intersections is too far or the relevance of traffic flow is too weak, uncoordinated signals should be utilized. Otherwise, coordinated signals should be adopted. Therefore, the optimization models with uncoordinated and coordinated signals were separately formulated for paired intersections with left-turn bays [21, 22]. A great number of research is aimed at optimizing offset setting to obtain the optimum effect of signal coordination. The typical methods can be divided into maximal bandwidth approach [23, 24] and delay minimization approach [25, 26]. A limited number of studies mentioned the suitable intersection spacing for signal coordination. The *Guidelines for Traffic Signals* (*RiLSA*) indicated that "*Green Waves for motorized traffic are recommended for a traffic signal spacing of up to 750 meters, or under particularly favorable conditions up to 1000 meters*" [27]. However, Roess et al. [28] denoted that "*common practice is to coordinate signals less than one mile apart on major streets and highways*."

In reality, the effects of signal coordination may be affected by many factors, such as intersection spacing, traffic demand, and platoon dispersion. If signal phasing for each intersection or the offset between paired intersections is not suitable in practice, the effects of signal coordination may be worse than those of no signal coordination. As stated before, a limited number of literature gave extremely different recommendation values for intersection spacing in the condition of which paired intersections should be coordinated. On the other hand, the provision of left-turn bays can enhance intersection operations, but then a lot of factors (e.g., intersection layout, traffic demand, signal phasing, and signal timings) need to be considered for which the performance of each left-turn bay can be maximized with the concern of multiperiod traffic design. When integrating the provision of left-turn bays and the applicability of signal coordination, little research investigates the related issues. This paper aims at covering these gaps. The optimization models with uncoordinated and coordinated signals and with the concern of left-turn bays are reformulated, respectively, under the same research framework. Some numerical examples and simulation experiments are carried out to analyze the impacts of different influencing factors on traffic flow operations.

The rest of this article is organized as below: in Section 2, the basic assumptions and the calculation of capacity and delay are presented together with the constraints. Then, the optimization models with uncoordinated and coordinated signals are reformulated by considering the uniform delay progression adjustment. In Section 3, numerical examples are given to demonstrate the application of the formulated models, and the sensitivities of the optimization results to different influencing factors are analyzed. In Section 4, the orthogonal experiments are designed and the obtained temporal-spatial resource allocation schemes are testified using the *VISSIM* software. In Section 5, the impacts of several parameters (e.g., initial queue and number of vehicles in a platoon) on the performance of the proposed models are discussed, and some suggestions are proposed together with the usage of the models in practice. In the last section, the achievements and contributions of this article are concluded.

## 2. Proposed Methodology

*2.1. Basic Assumptions.* This article aims at optimally allocating the temporal-spatial resources for paired intersections when left-turn bays may be provided. The following assumptions need to be satisfied:

(i) The studied paired intersections are both controlled by pretimed signals during peak periods

(ii) The saturation flow rate for each lane group can be estimated, and the peak 15 min flow rate and hourly volume can be collected during peak periods

(iii) One or more left-turn bays may be provided for left turns, and right turns on red are allowed at all approaches

Figure 1(a) shows the common geometric configuration for a pair of four-leg intersections. At each approach, one left-turn bay, one exclusive left-turn lane, one through lane, and one shared through-right lane are provided. Three important spatial parameters, i.e., left-turn bay length, intersection spacing, and length of the common road section, are specifically denoted.

The dual-ring structure is a commonly used method to design the signal phase plan for an intersection [28].

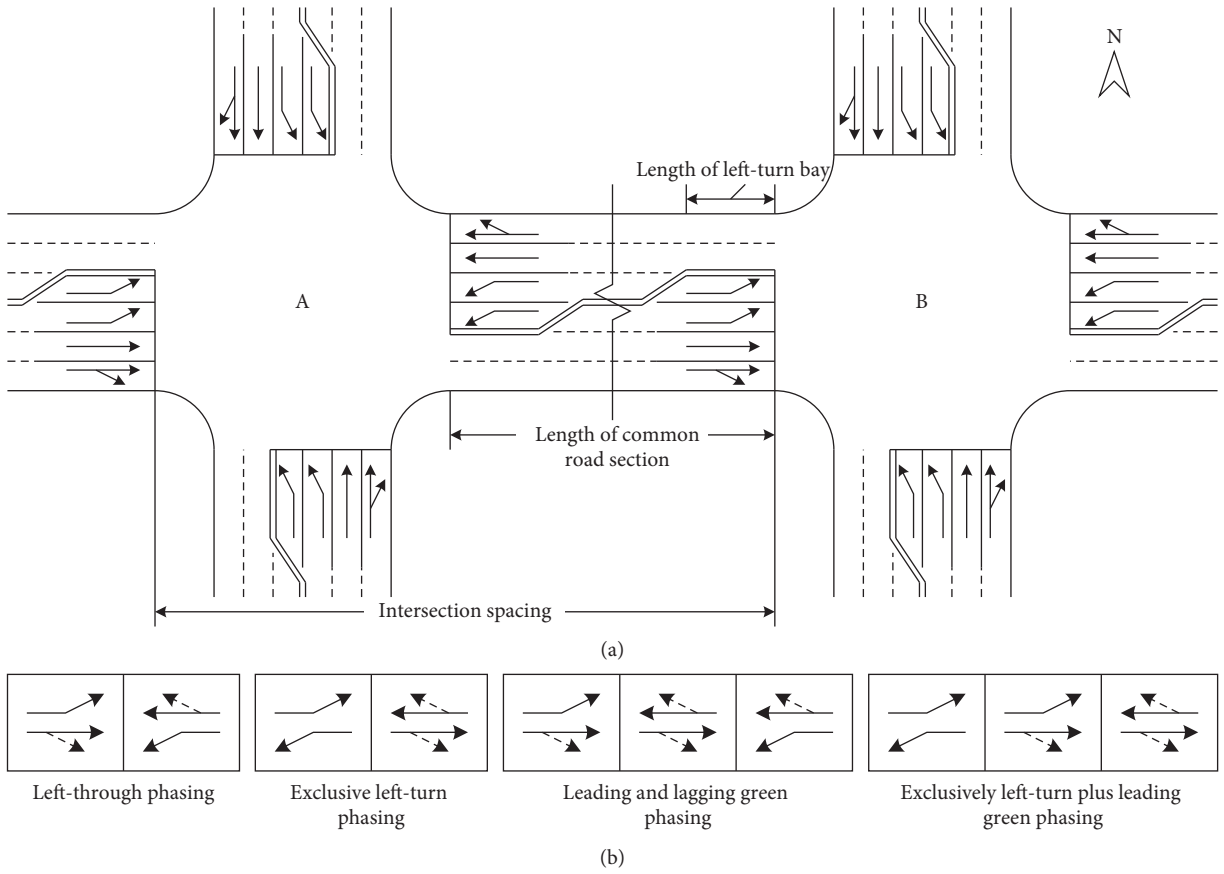


Figure 1: Geometric configuration (a) and signal phasing in each ring (b) at paired intersections.

For each ring (i.e., the east-west or south-north direction) at each intersection, Figure 1(b) shows the four possible combinations of signal phasing, that is, left-through phasing, exclusive left-turn phasing, leading and lagging green phasing, and exclusively left-turn plus leading green phasing [20]. Left-through phasing means that the subject left-turn and through movements simultaneously have or lose right-of-way, whereas exclusive left-turn phasing means that the subject and opposing left-turn movements simultaneously have or lose right-of-way. Leading green means that the subject left-turn movement goes before the opposing through movement, whereas lagging green means that the subject left-turn movement goes behind the opposing through movement.

At each approach, the number of exclusive left-turn or through lanes can be more than one, or there may be no left-turn bay. The illustrated case can also be simplified to consider one-way streets or three-leg intersections, and accordingly, the signal phase plans may be simpler. On the contrary, one or more shared left-through lanes may be provided, and in this case, permitted left-turn phasing should be designed. For all the abovementioned cases, the formulated models can still be used. However, because it is more difficult to accurately estimate the saturation flow rate for a shared left-through lane, the optimization results may not be ideal.

*2.2. Reduction of Saturation Flow Rate.* When left-turn or right-turn bays are provided on an intersection approach, they can only be efficiently used for a limited amount of time after the start of green, and setting the maximum green too high will result in loss of efficiency [11]. Figure 2 depicts the effects of a left-turn bay on the saturation flow rate for the lane group. As shown in Figure 2(a), the left-turn bay length is comprised of the queue storage length ($Q$), the length for full deceleration ($D_1$), and the taper length ($D_2$) [16]. Since the taper length is usually very short, the effective left-turn bay length ($D = Q + D_1$) is used to calculate the saturation flow rate for the lane group in this article. It is assumed that the left-turn traffic goes together with the through traffic at the same approach. As indicated in Figure 2(b), there is no overflow of left-turn bay and there is no blockage of the entrance by the queued vehicles in the adjacent through lane [17]. In Figure 2(c), the vehicles overflow in the left-turn bay; and in Figure 2(d), the entrance of the left-turn bay is blocked by the queued vehicles in the adjacent through lane. In any case of Figures 2(b)~2(d), the saturation flow rate of the lane group may not be constant but drops from a higher value to a lower value [3].

*2.3. Capacity and Delay.* Two common performance indices, i.e., capacity and delay, are usually considered for evaluating signal timings.

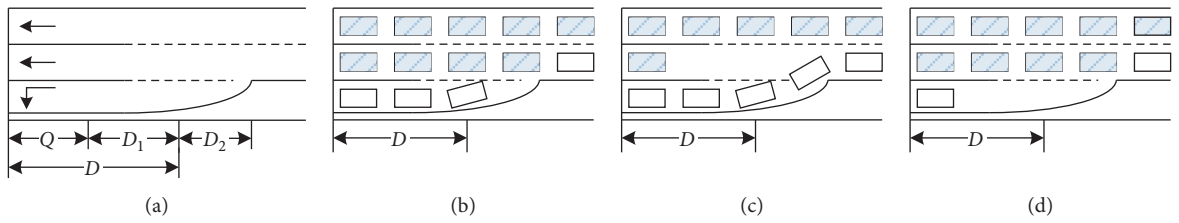


Figure 2: Influence of a left-turn bay on traffic operations. (a) Components. (b) No overflow and blockage. (c) Overflow. (d) Blockage.

The capacity of an intersection lane group is generally defined as the maximum hourly rate at which vehicles can reasonably be expected to pass through the stopline under prevailing traffic, roadway, and signalization conditions [1]. Due to the reduction of the saturation flow rate [3], the capacity of a lane group can be computed as

$$Q_j^\eta = \begin{cases} \dfrac{1}{C^\eta}\left(SF_j^\eta \sum_{i=1}^{n^\eta} \varphi_{ij}^\eta g_i^\eta + \dfrac{t}{h}\phi_j^\eta SS_j^\eta D_j^\eta\right), & \sum_{i=1}^{n^\eta} \varphi_{ij}^\eta g_i^\eta \geq \dfrac{t}{h} D_j^\eta, \\ \dfrac{1}{C^\eta}\left(SF_j^\eta + \phi_j^\eta SS_j^\eta\right) \sum_{i=1}^{n^\eta} \varphi_{ij}^\eta g_i^\eta, & \sum_{i=1}^{n^\eta} \varphi_{ij}^\eta g_i^\eta < \dfrac{t}{h} D_j^\eta, \end{cases} \tag{1}$$

where $\eta \in \{A, B\}$; $C^\eta = \sum_{i=1}^{n^\eta} g_i^\eta + L^\eta$; $Q_j^\eta$ is the capacity of lane group $j$ at intersection $\eta$ (pcu/h); $SF_j^\eta$ and $SS_j^\eta$ are the saturation flow rates for the normal lanes and for the left-turn bay in lane group $j$ at intersection $\eta$, respectively (pcu/h); $\varphi_{ij}^\eta$ is an identifier indicating whether vehicles in lane group $j$ can pass through the stopline in phase $i$ at intersection $\eta$, $\varphi_{ij}^\eta = 1$ if yes, or $\varphi_{ij}^\eta = 0$ if no; $\phi_j^\eta$ is an identifier indicating whether one left-turn bay is provided in lane group $j$ at intersection $\eta$, $\phi_j^\eta = 1$ if yes, or $\phi_j^\eta = 0$ if no; $D_j^\eta$ is the left-turn bay length for lane group $j$ at intersection $\eta$ (m); $C^\eta$ and $L^\eta$ are the cycle length and total lost time for intersection $\eta$, respectively (s); $n^\eta$ is the number of phases for intersection $\eta$; $g_i^\eta$ is the effective green time for phase $i$ at intersection $\eta$ (s); $t$ is the average saturation headway between consecutive vehicles (s); and $h$ is the average queue spacing between consecutive vehicles (m).

Then, the capacity of a given intersection is the summation of the capacities of all the lane groups, i.e.,

$$Q^\eta = \sum_{j=1}^{m^\eta} Q_j^\eta, \tag{2}$$

where $Q^\eta$ is the capacity of intersection $\eta$ (pcu/h) and $m^\eta$ is the number of lane groups for intersection $\eta$.

The average delay for a lane group can be given by [1]

$$d_j^\eta = \frac{0.5C^\eta\left(1-u_j^\eta\right)^2 PF_j^\eta}{1-\min\left(1, x_j^\eta\right)u_j^\eta} + 900T\left[\left(x_j^\eta - 1\right) + \sqrt{\left(x_j^\eta - 1\right)^2 + \frac{8KI_j^\eta x_j^\eta}{Q_j^\eta T}}\right] + \frac{3600}{q_j^\eta T}\left[\frac{\widetilde{t}_j^\eta\left(\widetilde{Q}_j^\eta + \widehat{Q}_j^\eta - \widehat{Q}_j^\eta\right)}{2} + \frac{\left(\widehat{Q}_j^\eta\right)^2 - \left(\widehat{Q}_j^\eta\right)^2}{2Q_j^\eta} - \frac{\left(\widetilde{Q}_j^\eta\right)^2}{2Q_j^\eta}\right], \tag{3}$$

where $\widetilde{t}_j^\eta = \begin{cases} \min\left\{T, \widetilde{Q}_j^\eta/(Q_j^\eta - q_j^\eta)\right\} & q_j^\eta < Q_j^\eta \\ T & q_j^\eta \geq Q_j^\eta \end{cases}$;

$\widehat{Q}_j^\eta = \begin{cases} 0 & q_j^\eta < Q_j^\eta \\ T(q_j^\eta - Q_j^\eta) & q_j^\eta \geq Q_j^\eta \end{cases}$; $\widehat{Q}_j = \widetilde{Q}_j^\eta + \widetilde{t}_j^\eta(q_j^\eta - Q_j^\eta)$; $x_j^\eta = q_j^\eta/Q_j^\eta$; $u_j^\eta = (1/C^\eta)(\sum_{i=1}^{n^\eta} \varphi_{ij}^\eta g_i^\eta)$; $d_j^\eta$ is the average delay for lane group $j$ at intersection $\eta$ (s/pcu); $PF_j^\eta$ and $I_j^\eta$ are the uniform delay progression adjustment factor and upstream filtering or metering adjustment factor for lane group $j$ at intersection $\eta$, respectively; $u_j^\eta$ and $x_j^\eta$ are the split and degree of saturation for lane group $j$ at intersection $\eta$, respectively; $q_j^\eta$ is the demand flow rate for lane group $j$ at intersection $\eta$ (pcu/h); $T$ is the analysis period (h); $K$ is the incremental delay factor for controller settings; $\widetilde{Q}_j^\eta$ and $\widetilde{t}_j^\eta$ are the initial queue (pcu) and duration of unmet demand (h) for lane group $j$ at intersection $\eta$, respectively; and $\widehat{Q}_j^\eta$ and $\widehat{Q}_j^\eta$ are the queue at the end of the analysis period (pcu) and queue at the end of the analysis period when $q_j^\eta \geq Q_j^\eta$ and $\widetilde{Q}_j^\eta = 0$ (pcu) for lane group $j$ at intersection $\eta$, respectively; each upstream filtering or metering adjustment factor is ascertained based on the literature [1].

During an analysis period, the total delay for a given intersection can be gotten by aggregating the average delays for all the lane groups, i.e.,

$$D^\eta = T\sum_{j=1}^{m^\eta} d_j^\eta q_j^\eta, \tag{4}$$

where $D^\eta$ is the total delay for intersection $\eta$ (s).

*2.4. Consideration of Constraints.* The following constraints have to be satisfied to obtain a reasonable signal timing plan.

First of all, the effective green time for each lane group should not be less than the queue full discharge time for the

left-turn bay so that the overflow and blockage of the left-turn bay can be effectively avoided; thus

$$\sum_{i=1}^{n^\eta} \varphi_{ij}^\eta g_i^\eta \geq \frac{t}{h} D_j^\eta, \quad \phi_j^\eta = 1. \tag{5}$$

Secondly, the effective green time for each lane group should not be less than a lower bound:

$$\sum_{i=1}^{n^\eta} \varphi_{ij}^\eta g_i^\eta \geq g_{\min}, \tag{6}$$

where $g_{\min}$ is the minimal effective green time (s).

Thirdly, the cycle length should be within the critical upper and lower bounds, namely,

$$C_{\min} \leq \sum_{i=1}^{n^\eta} g_i^\eta + L^\eta \leq C_{\max}, \tag{7}$$

where $C_{\min}$ is the minimal cycle length (s) and $C_{\max}$ is the maximal cycle length (s).

Fourthly, the lengths of the left-turn bays on the common road section should satisfy the following:

$$\begin{aligned} \phi_k^{\mathrm{A}} D_k^{\mathrm{A}} + \phi_l^{\mathrm{B}} D_l^{\mathrm{B}} &\leq D_0, \\ \delta_k^{\mathrm{A}} &= 1, \\ \delta_l^{\mathrm{B}} &= 1, \\ k &\in \left\{1, 2, 3, \ldots, m^{\mathrm{A}}\right\}, \\ l &\in \left\{1, 2, 3, \ldots, m^{\mathrm{B}}\right\}, \end{aligned} \tag{8}$$

where $\phi_k^{\mathrm{A}}$ and $\phi_l^{\mathrm{B}}$ are the identifiers indicating whether one left-turn bay is provided in lane group $k$ at intersection A and in lane group $l$ at intersection B, respectively, if yes $\phi_k^{\mathrm{A}} = 1$ and $\phi_l^{\mathrm{B}} = 1$, otherwise $\phi_k^{\mathrm{A}} = 0$ and $\phi_l^{\mathrm{B}} = 0$; $D_k^{\mathrm{A}}$ and $D_l^{\mathrm{B}}$ are the left-turn bay lengths for lane group $k$ at intersection A and for lane group $l$ at intersection B, respectively (m); $D_0$ is the length of the common road section (m); $\delta_k^{\mathrm{A}}$ and $\delta_l^{\mathrm{B}}$ are the identifiers indicating whether lane group $k$ at intersection A and lane group $l$ at intersection B are located on the common road section, respectively, if yes $\delta_k^{\mathrm{A}} = 1$ and $\delta_l^{\mathrm{B}} = 1$, otherwise $\delta_k^{\mathrm{A}} = 0$ and $\delta_l^{\mathrm{B}} = 0$; and $m^{\mathrm{A}}$ and $m^{\mathrm{B}}$ are the number of lane groups for intersections A and B, respectively. When $\phi_k^{\mathrm{A}} = 0$ and $\phi_l^{\mathrm{B}} = 0$, such a constraint does not exist.

Fifthly, the effective green time for each signal phase may not be negative, i.e.,

$$g_i^\eta \geq 0. \tag{9}$$

When the effective green time for a signal phase is equal to zero, this signal phase does not exist actually.

Sixthly, the length of each left-turn bay may also not be negative, that is,

$$\begin{aligned} D_j^\eta &\geq 0, \\ \phi_j^\eta &= 1. \end{aligned} \tag{10}$$

If the length of a left-turn bay equals zero, this left-turn bay does actually not need to be installed.

When coordinated signals are considered for paired intersections, all signals should have the same cycle length, and the offset should be equal to or larger than 0 and be less than the common cycle length. Therefore, the following two constraints need to be added:

$$\sum_{i=1}^{n^\eta} g_i^\eta + L^\eta = C_{\mathrm{c}}, \tag{11}$$

$$0 \leq o_{\mathrm{BA}} < \sum_{i=1}^{n^\eta} g_i^\eta + L^\eta, \tag{12}$$

where $C_{\mathrm{c}}$ is the common cycle length (s) and $o_{\mathrm{BA}}$ is the offset between intersections B and A, i.e., difference between the green initiation time of the first phase at intersection B and that at intersection A (s).

*2.5. Optimization Models.* When either of paired intersections can be regarded as an isolated intersection, the uniform delay progression adjustment factor can be set to 1 for each lane group [1]. That is, the uniform delay progression adjustment factors in equation (3) are all equal constants. As stated earlier, the intersection capacity depends on the capacity of each lane group. Since the average delay for a given lane group also depends on the capacity of the lane group, the total delay for the entire intersection depends on the capacity of each lane group. To optimally allocate the temporal-spatial resources, the total delay for paired intersections should be regarded as the objective function of the formulated optimization model. Certainly, the aforementioned constraints need to be satisfied. In this case, such a model can be expressed as

$$\begin{aligned} &\text{Minimize,} && \sum_{\eta \in \{\mathrm{A},\mathrm{B}\}} D^\eta = f\left(g_i^{\mathrm{A}}, D_j^{\mathrm{A}}, g_i^{\mathrm{B}}, D_j^{\mathrm{B}}\right), \\ &\text{Subject to,} && \text{Eqs. (5) } \sim \text{ (10),} \end{aligned} \tag{13}$$

where $f\left(g_i^{\mathrm{A}}, D_j^{\mathrm{A}}, g_i^{\mathrm{B}}, D_j^{\mathrm{B}}\right)$ is the function of variables $g_i^{\mathrm{A}}$, $D_j^{\mathrm{A}}$, $g_i^{\mathrm{B}}$, and $D_j^{\mathrm{B}}$.

Equation (13) is one nonlinear single-objective optimization problem with linear inequality constraints and can be solved using the *fmincon* function in the *MATLAB* software. This model is denoted by Model US (uncoordinated signals).

When either of paired intersections could not be viewed as an isolated intersection, these two intersections need to be coordinated. In other words, coordinated signals have to be considered, and some uniform delay progression adjustment factors in equation (3) are not constants.

According to HCM 2010 [1], the uniform delay progression adjustment factor should be set to 1 for all uncoordinated lane groups and movements released from exclusive left-turn lanes in exclusive phases, whereas the uniform delay progression adjustment factor for coordinated lane groups can be written as

$$PF_j^\eta = \min\left\{1, \frac{\left[\left(1 - P_j^\eta\right)\widetilde{f}_j^\eta\right]}{\left(1 - u_j^\eta\right)}\right\}, \tag{14}$$

where $P_j^\eta$ and $\widetilde{f}_j^\eta$ are the proportion of vehicles arriving on green and supplemental adjustment factor for platoon arrival for lane group $j$ at intersection $\eta$, respectively.

The supplemental adjustment factor for platoon arrival during the green phase can be set to [1]

$$\widetilde{f}_j^\eta = \begin{cases} 0.93, & 0.50 < \widetilde{r}_j^\eta \le 0.85, \\ 1.15, & 1.15 < \widetilde{r}_j^\eta \le 1.50, \\ 1, & \text{else}, \end{cases} \tag{15}$$

where $\widetilde{r}_j^\eta = P_j^\eta / u_j^\eta$ and $\widetilde{r}_j^\eta$ is the platoon ratio for lane group $j$ at intersection $\eta$.

Reading the related study [29] for reference, the proportion of vehicles arriving on green can be given by

$$P_j^\eta = \begin{cases} 1 - \dfrac{q_j^\eta \tau_j^\eta}{\left(3600 N_j^\eta\right)}, & N_j^\eta \le \dfrac{q_j^\eta \left(\tau_j^\eta + \widetilde{g}_j^\eta\right)}{3600}, \quad o^\eta + \widetilde{g}_j^\eta \le O^\eta < o^\eta + C_c, \\ \dfrac{q_j^\eta \widetilde{g}_j^\eta}{\left(3600 N_j^\eta\right)}, & N_j^\eta > \dfrac{q_j^\eta \left(\tau_j^\eta + \widetilde{g}_j^\eta\right)}{3600}, \quad o^\eta + \widetilde{g}_j^\eta \le O^\eta < o^\eta + C_c, \\ 1 - \dfrac{q_j^\eta \widetilde{\tau}_j^\eta}{\left(3600 N_j^\eta\right)}, & \widetilde{\tau}_j^\eta < r_j^\eta + \dfrac{q_j^\eta r_j^\eta}{\left(S_j^\eta - q_j^\eta\right)}, \quad o^\eta \le O^\eta < o^\eta + \widetilde{g}_j^\eta, \\ 1 - \dfrac{q_j^\eta r_j^\eta}{\left(3600 N_j^\eta\right)}, & \widetilde{\tau}_j^\eta \ge r_j^\eta + \dfrac{q_j^\eta r_j^\eta}{\left(S_j^\eta - q_j^\eta\right)}, \quad o^\eta \le O^\eta < o^\eta + \widetilde{g}_j^\eta, \end{cases} \tag{16}$$

where $S_j^\eta = \begin{cases} \left(SF_j^\eta \widetilde{g}_j^\eta + t\phi_j^\eta SS_j^\eta D_j^\eta / h\right) / \widetilde{g}_j^\eta, & \widetilde{g}_j^\eta \ge (t/h) D_j^\eta, \\ SF_j^\eta + \phi_j^\eta SS_j^\eta, & \widetilde{g}_j^\eta \ge (t/h) D_j^\eta. \end{cases}$; $\tau_j^\eta = C_c - O^\eta + o^\eta$; $\widetilde{g}_j^\eta = \sum_{i=1}^{n^\eta} \varphi_{ij}^\eta g_i^\eta$; $r_j^\eta = C_c - \widetilde{g}_j^\eta$; $\widetilde{\tau}_j^\eta = 3600 N_j^\eta / q_j^\eta + O^\eta - o^\eta - \widetilde{g}_j^\eta$; $N_j^\eta$ is the number of vehicles in a platoon for lane group $j$ at intersection $\eta$ (pcu); $S_j^\eta$ is the equivalent saturation flow rate for lane group $j$ at intersection $\eta$ (pcu/h); $\tau_j^\eta$ and $\widetilde{\tau}_j^\eta$ are the difference between the arrival time of the first vehicle and the end of red and the difference between the arrival time of the last vehicle and the start of red for lane group $j$ at intersection $\eta$, respectively (s); $O^\eta$ and $o^\eta$ are the ideal and actual offsets between intersection $\eta$ and the upstream intersection, respectively (s); and $\widetilde{g}_j^\eta$ and $r_j^\eta$ are the effective green time and effective red time for lane group $j$ at intersection $\eta$, respectively (s).

Based on the previous studies [22, 28], the ideal and actual offsets can be expressed as

$$O^\eta = \begin{cases} \mathrm{mod}\left(\dfrac{s_{BA}}{v_{BA}}, C_c\right), & \mathrm{mod}\left(\dfrac{s_{BA}}{v_{BA}}, C_c\right) \ge o^\eta, \quad \eta = \mathrm{A}, \\ \mathrm{mod}\left(\dfrac{s_{BA}}{v_{BA}}, C_c\right) + C_c, & \mathrm{mod}\left(\dfrac{s_{BA}}{v_{BA}}, C_c\right) < o^\eta, \quad \eta = \mathrm{A}, \\ \mathrm{mod}\left(\dfrac{s_{AB}}{v_{AB}}, C_c\right), & \mathrm{mod}\left(\dfrac{s_{AB}}{v_{AB}}, C_c\right) \ge o^\eta, \quad \eta = \mathrm{B}, \\ \mathrm{mod}\left(\dfrac{s_{AB}}{v_{AB}}, C_c\right) + C_c, & \mathrm{mod}\left(\dfrac{s_{AB}}{v_{AB}}, C_c\right) < o^\eta, \quad \eta = \mathrm{B}, \end{cases} \tag{17}$$

$$o^\eta = \begin{cases} C_c - o_{BA} + \mathrm{ON}_A - \mathrm{ON}_B, & \eta = \mathrm{A}, \\ o_{BA} - \mathrm{OP}_A + \mathrm{OP}_B, & \eta = \mathrm{B}, \end{cases}$$

where $\mathrm{mod}(s_{BA}/v_{BA}, C_c)$ is the remainder of $s_{BA}/v_{BA}$ divided by $C_c$ (s); $s_{BA}$ is the distance between the stopline at intersection B and that at intersection A (m); $v_{BA}$ is the average running speed of a platoon from intersections B to A (m/s); $\mathrm{mod}(s_{AB}/v_{AB}, C_c)$ is the remainder of $s_{AB}/v_{AB}$ divided by $C_c$ (s); $s_{AB}$ is the distance between the stopline at intersection A and that at intersection B (m); $v_{AB}$ is the average running speed of a platoon from intersections A to B (m/s); $OP_A$ and $OP_B$ are the difference between the green initiation time for the coordinated phase and that for the first phase in the positive direction at intersections A and B, respectively (s); and $ON_A$ and $ON_B$ are the difference between the green initiation time for the coordinated phase and that for the first phase in the negative direction at intersections A and B, respectively (s).

Because the uniform delay progression adjustment factor for each lane group may be a function of the offset between paired intersections, the total delays for each intersection and for paired intersections are both the functions of the offset between paired intersections. When minimizing the total delay for paired intersections under the constraints, the optimization model becomes

$$\begin{aligned} &\text{Minimize,} && \sum_{\eta\in\{A,B\}} D^{\eta} = f\left(g_i^A, D_j^A, g_i^B, D_j^B, o_{BA}\right), \\ &\text{Subject to,} && \text{Eqs. (5) } \sim \text{ (12),} \end{aligned} \tag{18}$$

where $f(g_i^A, D_j^A, g_i^B, D_j^B, o_{BA})$ is the function of variables $g_i^A$, $D_j^A$, $g_i^B$, $D_j^B$, and $o_{BA}$.

Similarly, equation (18) is a nonlinear single-objective optimization problem with linear inequality and equality constraints and can be solved using the *fmincon* function. This model is denoted by Model CS (coordinated signals).

## 3. Numerical Examples

*3.1. Traffic Data.* For paired intersections shown in Figure 1(a), three levels of traffic demands are assumed, i.e., low, median, and high levels. Concerning left-turn, through, and right-turn traffic on each approach, traffic volumes in a 15 min interval are randomly generated from 140 to 170, from 110 to 140, and from 20 to 40, respectively, under the low level; they range from 150 to 180, from 120 to 150, and from 30 to 50, respectively, under the median level; and they range from 160 to 190, from 130 to 160, and from 40 to 60, respectively, under the high level; where the unit of traffic volume is pcu/15 mins. The hourly volume for each movement equals the sum of the produced traffic volumes in four successive 15 min intervals. The peak 15 min flow rate for each movement equals 4 times as much as the maximum of the produced traffic volumes in four successive 15 min intervals. The three sets of traffic demand samples are listed in Table 1. Based on such traffic demands, the signal phase plans for intersections A and B are designed in view of our previous study [19], as pictured in Figure 3. In this figure, M1, M3, M5, and M7 represent the eastbound, southbound, westbound, and northbound left-turn movements, respectively; M2, M4, M6 and M8 represent the westbound, northbound, eastbound, and southbound through movements, respectively.

*3.2. Parameter Calibration.* The saturation flow rates for all the lane groups herein are assumed on the basis of ideal conditions as mentioned by Akçelik [3]; specifically, environment class A and lane types 1 and 2. Environment class A means ideal or nearly ideal conditions in which each vehicle movement on an approach or exit is free, such as good visibility, very few pedestrians, and almost no interference resulted from loading or unloading goods or parking. Lane type 1 represents a through lane, i.e., a lane which contains through vehicles only. Lane type 2 refers to a turning lane including an exclusive left-turn or right-turn lane, or a shared left-through, and through-right or left-through-right lane, i.e., a lane which contains any type of turning traffic. Moreover, turning vehicles are subject to adequate radius and negligible pedestrian interference. Therefore, the saturation flow rates for an exclusive left-turn lane, a through lane, and a shared through-right lane are assumed to be 1810, 1850, and 1810 pcu/h, respectively [3]. The average lost time per phase transition is 3 s, the average saturation headway between successive vehicles is 2 s, and the average queue spacing between successive vehicles is 6 m [30]. The signal phasing for each intersection adopts the dual-ring structure, and the number of discrete phases is the number of phase transition in a signal cycle in each ring, i.e., 4 [28]. For each lane group, the minimal effective green time, amber time, and all-red time are 10, 3, and 2 s, respectively [27]. For each intersection, the minimal and maximal cycle lengths are 60 and 150 s, respectively [1].

The duration of analysis period is assumed to be 1 h. The paired intersections are assumed to be controlled by pretimed signals; thus, the incremental delay factor is 0.5 for each lane group. It is assumed that there is no initial queue in each lane group at the start of the analysis period, meaning no initial queue delay for each lane group. The number of vehicles in a platoon adopts 20 pcu for each coordinated movement. The average running speed of a platoon is 50 km/h on the arterial street. Additionally, the distance between the stoplines for the subject and opposing coordinated movements is assumed to be 45 m at each intersection.

*3.3. Sensitivity Analysis.* To compare the performance of Models US and CS, i.e., equations (13) and (18), the geometric configuration in Figure 1(a) and the traffic demand data in Table 1 are used, and the spacing between paired intersections varies from 245 to 1645 m (i.e., the length of the common road section varies from 200 to 1600 m) with a 100 m increment. Then, the formulated two optimization models are tested over and over again. As a result, a total of 90 sets of optimization outcomes are obtained, where 20 decision variables of Model US, 21 decision variables of Model CS, and 9 performance indices for each model are involved. The decision variables include the effective green time per phase, the offset between paired intersections, and the length for each left-turn bay; and the performance indices include the capacity, delay, average delay, degree of

Table 1: Three levels of traffic demands.

| Level of demand | Approach | Movement | Intersection A | | Intersection B | |
|---|---|---|---|---|---|---|
| | | | Hourly volume (pcu/h) | Peak 15 min flow rate (pcu/h) | Hourly volume (pcu/h) | Peak 15 min flow rate (pcu/h) |
| Low | Eastbound | Left-turn | 629 | 676 | 626 | 652 |
| | | Through | 483 | 520 | 483 | 505 |
| | | Right-turn | 118 | 152 | 108 | 151 |
| | Southbound | Left-turn | 611 | 652 | 600 | 628 |
| | | Through | 473 | 544 | 488 | 540 |
| | | Right-turn | 125 | 132 | 111 | 156 |
| | Westbound | Left-turn | 590 | 621 | 628 | 668 |
| | | Through | 496 | 539 | 474 | 504 |
| | | Right-turn | 107 | 124 | 124 | 156 |
| | Northbound | Left-turn | 628 | 656 | 608 | 624 |
| | | Through | 526 | 560 | 501 | 544 |
| | | Right-turn | 123 | 136 | 127 | 156 |
| Median | Eastbound | Left-turn | 670 | 716 | 671 | 701 |
| | | Through | 548 | 588 | 524 | 572 |
| | | Right-turn | 162 | 200 | 164 | 195 |
| | Southbound | Left-turn | 660 | 688 | 641 | 716 |
| | | Through | 549 | 600 | 505 | 560 |
| | | Right-turn | 148 | 168 | 157 | 172 |
| | Westbound | Left-turn | 654 | 670 | 674 | 704 |
| | | Through | 516 | 559 | 505 | 536 |
| | | Right-turn | 151 | 175 | 159 | 196 |
| | Northbound | Left-turn | 670 | 712 | 659 | 696 |
| | | Through | 539 | 572 | 561 | 592 |
| | | Right-turn | 151 | 192 | 162 | 196 |
| High | Eastbound | Left-turn | 669 | 688 | 669 | 708 |
| | | Through | 573 | 588 | 589 | 599 |
| | | Right-turn | 186 | 196 | 177 | 189 |
| | Southbound | Left-turn | 658 | 676 | 707 | 760 |
| | | Through | 580 | 636 | 581 | 640 |
| | | Right-turn | 199 | 224 | 177 | 204 |
| | Westbound | Left-turn | 654 | 699 | 706 | 744 |
| | | Through | 586 | 606 | 572 | 608 |
| | | Right-turn | 202 | 239 | 183 | 204 |
| | Northbound | Left-turn | 683 | 704 | 693 | 732 |
| | | Through | 580 | 612 | 572 | 640 |
| | | Right-turn | 204 | 232 | 227 | 236 |

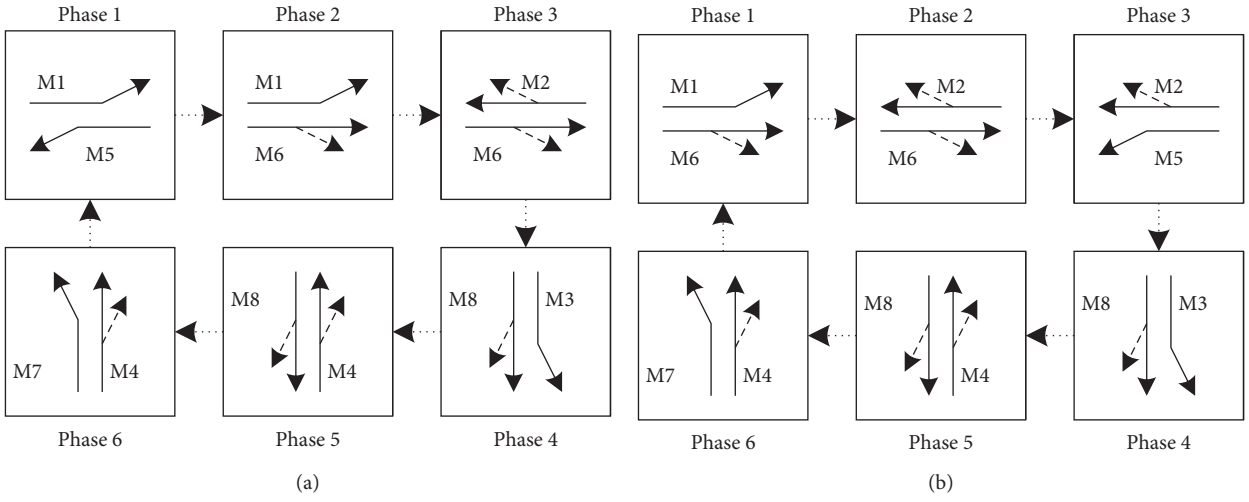


Figure 3: Specific signal phase plans. (a) Intersection A. (b) Intersection B.

Table 2: Optimization results for ninety numerical examples.

| Model | Demand | Spacing (m) | Effective green times for intersection A (s) | | | | | | Offset (s) | Left-turn bay lengths for intersection A (m) | | | |
|---|---|---|---|---|---|---|---|---|---|---|---|---|---|
| | | | Phase 1 | Phase 2 | Phase 3 | Phase 4 | Phase 5 | Phase 6 | | Eastbound | Southbound | Westbound | Northbound |
| US | Low | 245 | 14.54 | 0.70 | 14.81 | 14.86 | 0.53 | 15.11 | — | 45.72 | 44.57 | 43.62 | 45.33 |
| US | Low | 345 | 14.54 | 0.70 | 14.81 | 14.86 | 0.53 | 15.11 | — | 45.72 | 44.57 | 43.62 | 45.33 |
| US | Low | 445 | 14.54 | 0.70 | 14.81 | 14.86 | 0.53 | 15.11 | — | 45.72 | 44.57 | 43.62 | 45.33 |
| ... | ... | ... | ... | ... | ... | ... | ... | ... | ... | ... | ... | ... | ... |
| CS | High | 1445 | 23.16 | 0.00 | 27.00 | 23.36 | 5.03 | 23.60 | 0 | 69.47 | 70.07 | 69.47 | 70.79 |
| CS | High | 1545 | 23.16 | 0.00 | 27.02 | 23.38 | 5.01 | 23.65 | 0 | 69.47 | 70.13 | 69.47 | 70.95 |
| CS | High | 1645 | 23.16 | 0.00 | 27.00 | 23.36 | 5.03 | 23.60 | 0 | 69.47 | 70.07 | 69.47 | 70.79 |
| Model | Demand | Spacing (m) | Effective green times for intersection B (s) | | | | | | Offset (s) | Left-turn bay lengths for intersection B (m) | | | |
| | | | Phase 1 | Phase 2 | Phase 3 | Phase 4 | Phase 5 | Phase 6 | | Eastbound | Southbound | Westbound | Northbound |
| US | Low | 245 | 14.71 | 0.00 | 14.94 | 14.19 | 1.38 | 14.19 | — | 44.14 | 42.57 | 44.82 | 42.56 |
| US | Low | 345 | 14.71 | 0.00 | 14.94 | 14.19 | 1.38 | 14.19 | — | 44.14 | 42.57 | 44.82 | 42.56 |
| US | Low | 445 | 14.71 | 0.00 | 14.94 | 14.19 | 1.38 | 14.19 | — | 44.14 | 42.57 | 44.82 | 42.56 |
| ... | ... | ... | ... | ... | ... | ... | ... | ... | ... | ... | ... | ... | ... |
| CS | High | 1445 | 23.00 | 2.09 | 24.40 | 24.62 | 3.39 | 24.64 | 106.55 | 68.99 | 73.85 | 73.20 | 73.93 |
| CS | High | 1545 | 23.01 | 2.09 | 24.43 | 24.63 | 3.39 | 24.66 | 55.30 | 69.04 | 73.89 | 73.28 | 73.99 |
| CS | High | 1645 | 23.00 | 2.09 | 24.40 | 24.62 | 3.39 | 24.64 | 107.99 | 68.99 | 73.85 | 73.20 | 73.93 |
| Model | Demand | Spacing (m) | Intersection A | | | | Intersection B | | | |
| | | | Capacity (pcu/h) | Delay (s) | Average delay (s/pcu) | Degree of saturation | Capacity (pcu/h) | Delay (s) | Average delay (s/pcu) | Degree of saturation |
| US | Low | 245 | 6076.26 | 182727.86 | 37.22 | 0.81 | 6057.41 | 180072.06 | 36.92 | 0.81 |
| US | Low | 345 | 6076.26 | 182727.86 | 37.22 | 0.81 | 6057.41 | 180072.06 | 36.92 | 0.81 |
| US | Low | 445 | 6076.26 | 182727.86 | 37.22 | 0.81 | 6057.41 | 180072.06 | 36.92 | 0.81 |
| ... | ... | ... | ... | ... | ... | ... | ... | ... | ... | ... |
| CS | High | 1445 | 6517.71 | 326951.51 | 56.62 | 0.89 | 6516.52 | 341106.02 | 58.28 | 0.90 |
| CS | High | 1545 | 6518.23 | 326984.33 | 56.63 | 0.89 | 6517.04 | 341198.07 | 58.29 | 0.90 |
| CS | High | 1645 | 6517.71 | 326951.51 | 56.62 | 0.89 | 6516.52 | 341106.02 | 58.28 | 0.90 |

saturation for each intersection, and the total delay for paired intersections. Table 2 lists the optimization results for the numerical examples. Because the data are too much, only some data are presented and the rest data are omitted.

The general linear model provided in the *SPSS* software is used to analyze the sensitivities of the optimized values of the decision variables and performance indices to the above three factors (i.e., optimization model, traffic demand, and intersection spacing). At 1% significance level, the findings indicate that the following: (1) the intersection spacing has no significant effects on all the decision variables and performance indices, whereas the traffic demand only has no significant effects on the offset between paired intersections; (2) the optimization model does not have significant impacts on all the effective green times, left-turn bay lengths, and performance indices but has significant impacts on the offset between paired intersections; and (3) the combination of the optimization model and intersection spacing has no significant effects on the optimization outcomes, whereas the combination of the optimization model and traffic demand and that of the traffic demand and intersection spacing both have significant impacts on the optimization outcomes.

The total delay for paired intersections is adopted to compare the performance of Models US and CS for each level of traffic demand. Herein, the total delay for paired intersections is defined as the sum of the total delay for each intersection calculated by equation (4). In this case, three paired scenarios are obtained and Student's $t$-tests are carried out. The left and right critical $t$ values are $-2.624$ and 2.624 at 1% significance level, respectively. If the calculated $t$ value for a paired scenario generated by Models US and CS is greater than the right critical $t$ value, Model CS performs better than Model US in view of the total delay for paired intersections. Figure 4 illustrates the results of Student's $t$-tests at 1% significance level for three levels of traffic demands when Model US is compared with Model CS. It can be seen that Model CS outstrips Model US for each level of traffic demand at 1% significance level; and the difference between these two models will be unobvious when traffic demand is low enough.

## 4. Simulation Experiments

*4.1. Orthogonal Experimental Scenarios.* To further verify the performance of Models US and CS, the *VISSIM* software is used to carry out the simulation tests. The version of *VISSIM*_6.00-19 is used here. The maximum network size licensed for this version of *VISSIM* is 1500 m for both the horizontal and vertical directions. Considering the reduction of workload and the limitation of the *VISSIM* edition, the orthogonal experiments are designed, as listed in Table 3. In this table, nine levels of intersection spacing which varies from 245 to 1045 m with a 100 m increment are given. The length of each left-turn bay adopts the listed value in the simulation model. The adopted left-turn bay length is the nearest integer times as much as the average queue spacing between consecutive vehicles and is not less than the maximum among the optimized values of all the left-turn bays obtained by utilizing Models US and CS. The signal timing plan for each experimental scenario adopts the signal timing plan obtained by utilizing the corresponding model under the same case, as indicated in Table 4. In this table, G1, G2, G3, G4, G5, G6, G7, and G8 refer to the displayed green time for M1, M2, M3, M4, M5, M6, M7, and M8, respectively; $C$ and $o$ are the cycle length and offset, separately.

In the simulation models, the Wiedemann 74 car following model is used and the simulation period is set to 4200 s. For exclusive left-turn, through, and shared through-right lanes, the additive parts of safety distance are set to 2.45, 2.40, and 2.45, respectively; and the multiplicative parts of safety distance are set to 3.45, 3.40, and 3.45, respectively. For each experimental scenario, the multirun mode is selected, and the initial random seed and increment of random seed are set to 5 and 10, respectively. Based on the *Guideline for Microscopic Traffic Simulation Analysis* [31], the warm-up time (also called system-initialization time) should be set in *VISSIM* before collecting the data for evaluation. Here the warm-up time is set to 600 s, and the simulation data are collected from 600 to 4200 s, i.e., in one hour. The other parameters use the default values.

At 95% confidence level, the expected confidence interval should be 1.50 times as much as the standard deviation [31], and the calculated confidence interval will be 1.43 times as much as the standard deviation if the number of runs adopts 10. To guarantee that the simulation outcomes are effective and sufficient, the expected value of the confidence interval needs to be greater than its calculated value [31]. Thus, the number of runs is set to 10 in this research.

*4.2. Simulation Results.* To evaluate the effectiveness of each experimental scenario, the travel time sections are installed for all the movements, and the distance between the starting and ending sections is 150 m for each travel time section. By aggregation, four performance indices can individually be provided for thirteen delay measurements. These four performance indices are the average stopped delay, number of stops, vehicle delay, and the vehicle throughput. These thirteen delay measurements include eight approaches, two intersections, two coordinated movements, and a pair of intersections. For the above eighteen scenarios, a total of 2,340 sets of data are obtained.

The acquired delay data are analyzed using the general linear model. The outcomes reveal the following: (1) the average stopped delay and vehicle delay are both impacted by the optimization model at 1% significance level, whereas both of them are not impacted by the delay measurement at the same level; (2) the vehicle throughput is not influenced by the intersection spacing at 1% significance level; (3) all the performance indices are impacted by the traffic demand at 1% significance level, whereas none of all the performance indices are influenced by the number of simulation runs at the same level.

Using the network performance evaluation, a total of 180 sets of sample data are obtained. Thirteen performance indices including the average delay, number of stops, speed, stopped delay, total distance, travel time, delay, number of stops, stopped delay, active and arrived vehicles, the latent

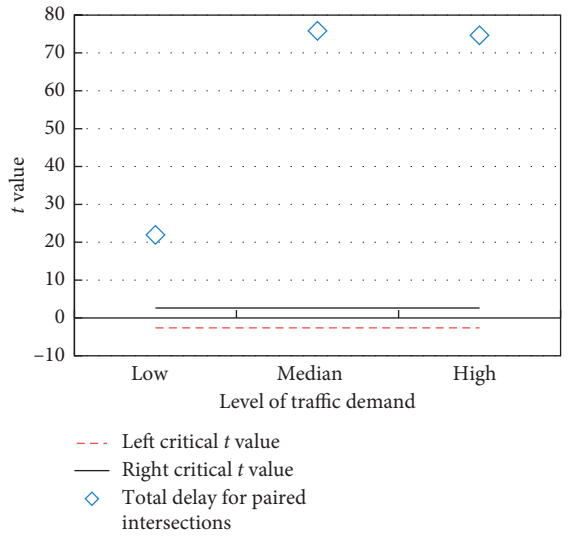


Figure 4: Results of Student's $t$-tests of total delay for paired intersections.

Table 3: Orthogonal experimental scenarios for traffic simulation.

| Test | Factors | | | |
|---|---|---|---|---|
| | Signal timing plan | Intersection spacing (m) | Level of demand | Length of left-turn bay (m) |
| 1<br>2 | Model US<br>Model CS | 245 | Low | 48 |
| 3<br>4 | Model US<br>Model CS | 345 | Median | 66 |
| 5<br>6 | Model US<br>Model CS | 445 | High | 84 |
| 7<br>8 | Model US<br>Model CS | 545 | Median | 66 |
| 9<br>10 | Model US<br>Model CS | 645 | High | 84 |
| 11<br>12 | Model US<br>Model CS | 745 | Low | 48 |
| 13<br>14 | Model US<br>Model CS | 845 | High | 84 |
| 15<br>16 | Model US<br>Model CS | 945 | Low | 48 |
| 17<br>18 | Model US<br>Model CS | 1045 | Median | 66 |

Table 4: Signal timing plans for traffic simulation.

| Test | Intersection | G1 (s) | G2 (s) | G3 (s) | G4 (s) | G5 (s) | G6 (s) | G7 (s) | G8 (s) | $C$ (s) | $o$ (s) |
|---|---|---|---|---|---|---|---|---|---|---|---|
| 1 | A | 13 | 13 | 13 | 14 | 13 | 13 | 13 | 14 | 73 | — |
| | B | 13 | 13 | 12 | 13 | 13 | 13 | 12 | 13 | 71 | — |
| 2 | A | 12 | 11 | 12 | 13 | 11 | 12 | 12 | 13 | 68 | 0 |
| | B | 11 | 12 | 12 | 13 | 12 | 11 | 12 | 13 | 68 | 62 |
| 3 | A | 18 | 19 | 18 | 20 | 17 | 20 | 18 | 20 | 95 | — |
| | B | 19 | 19 | 18 | 20 | 18 | 20 | 19 | 19 | 96 | — |
| 4 | A | 18 | 17 | 17 | 18 | 16 | 19 | 17 | 18 | 90 | 0 |
| | B | 17 | 18 | 17 | 18 | 17 | 18 | 17 | 18 | 90 | 23 |
| 5 | A | 21 | 25 | 21 | 26 | 21 | 25 | 21 | 26 | 113 | — |
| | B | 24 | 27 | 25 | 29 | 25 | 26 | 25 | 29 | 125 | — |
| 6 | A | 21 | 25 | 21 | 27 | 21 | 25 | 22 | 26 | 114 | 0 |
| | B | 21 | 24 | 23 | 26 | 22 | 23 | 23 | 26 | 114 | 102 |

Table 4: Continued.

| Test | Intersection | G1 (s) | G2 (s) | G3 (s) | G4 (s) | G5 (s) | G6 (s) | G7 (s) | G8 (s) | $C$ (s) | $o$ (s) |
|---|---|---|---|---|---|---|---|---|---|---|---|
| 7 | A | 18 | 19 | 18 | 20 | 17 | 20 | 18 | 20 | 95 | — |
| | B | 19 | 19 | 18 | 20 | 18 | 20 | 19 | 19 | 96 | — |
| 8 | A | 18 | 17 | 18 | 19 | 16 | 19 | 18 | 19 | 92 | 0 |
| | B | 17 | 18 | 18 | 19 | 17 | 18 | 18 | 19 | 92 | 55 |
| 9 | A | 21 | 5 | 21 | 26 | 21 | 25 | 21 | 26 | 113 | — |
| | B | 24 | 27 | 25 | 29 | 25 | 26 | 25 | 29 | 125 | — |
| 10 | A | 21 | 25 | 21 | 27 | 21 | 25 | 22 | 26 | 114 | 0 |
| | B | 21 | 24 | 23 | 26 | 22 | 23 | 23 | 26 | 114 | 91 |
| 11 | A | 13 | 13 | 13 | 14 | 13 | 13 | 13 | 14 | 73 | — |
| | B | 13 | 13 | 12 | 13 | 13 | 13 | 12 | 13 | 71 | — |
| 12 | A | 12 | 12 | 12 | 12 | 11 | 13 | 12 | 12 | 68 | 0 |
| | B | 11 | 12 | 12 | 13 | 12 | 11 | 12 | 13 | 68 | 0 |
| 13 | A | 21 | 25 | 21 | 26 | 21 | 25 | 21 | 26 | 113 | — |
| | B | 24 | 27 | 25 | 29 | 25 | 26 | 25 | 29 | 125 | — |
| 14 | A | 21 | 25 | 21 | 27 | 21 | 25 | 22 | 26 | 114 | 0 |
| | B | 21 | 24 | 23 | 26 | 22 | 23 | 23 | 26 | 114 | 110 |
| 15 | A | 13 | 13 | 13 | 14 | 13 | 13 | 13 | 14 | 73 | — |
| | B | 13 | 13 | 12 | 13 | 13 | 13 | 12 | 13 | 71 | — |
| 16 | A | 13 | 12 | 12 | 13 | 12 | 13 | 12 | 13 | 70 | 0 |
| | B | 12 | 13 | 12 | 13 | 13 | 12 | 12 | 13 | 70 | 68 |
| 17 | A | 18 | 19 | 18 | 20 | 17 | 20 | 18 | 20 | 95 | — |
| | B | 19 | 19 | 18 | 20 | 18 | 20 | 19 | 19 | 96 | — |
| 18 | A | 18 | 17 | 17 | 19 | 16 | 19 | 17 | 19 | 91 | 0 |
| | B | 17 | 18 | 17 | 19 | 17 | 18 | 18 | 18 | 91 | 34 |

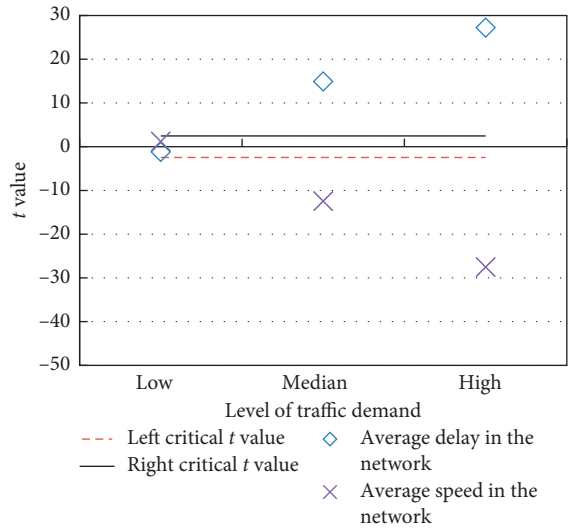


Figure 5: Results of Student's $t$-tests for average delay and speed in the network.

delay, and demand are provided. By adopting the general linear model, it can be shown that (1) the effects of the optimization model on all the performance indices are not significant at 1% significance level, (2) the impacts of the traffic demand on all the performance indices except the average number of stops are significant at 1% significance level, (3) the effects of the intersection spacing and the combination of the optimization model, traffic demand, and intersection spacing on all the performance indices except the latent demand are significant at 1% significance level, and (4) the influences of the number of simulation runs on the average number of stops, the latent delay, and the latent demand are significant at 1% significance level.

Two public factors are extracted from these thirteen performance indices by utilizing the factor analysis. Then, the average delay and speed in the network are both selected to compare the effects of the formulated optimization models on traffic flow operations. At this time, six paired scenarios are acquired and Student's $t$-tests are fulfilled. The left and right critical $t$ values are −2.462 and 2.462 at 1%

Table 5: Typical performance indices from traffic simulation.

| Test | Model | Demand | Spacing (m) | Average delay at paired intersections (s/pcu) | Average delay in the network (s/pcu) | Average speed in the network (km/h) |
|---|---|---|---|---|---|---|
| 1 | US | Low | 245 | 30.58 | 40.81 | 21.72 |
| 2 | CS | Low | 245 | 29.61 | 39.56 | 22.11 |
| 3 | US | Median | 345 | 38.76 | 51.98 | 20.54 |
| 4 | CS | Median | 345 | 37.63 | 50.34 | 20.91 |
| 5 | US | High | 445 | 45.29 | 60.72 | 20.14 |
| 6 | CS | High | 445 | 41.77 | 56.08 | 21.15 |
| 7 | US | Median | 545 | 38.03 | 51.04 | 22.34 |
| 8 | CS | Median | 545 | 37.18 | 49.79 | 22.65 |
| 9 | US | High | 645 | 45.26 | 60.56 | 21.52 |
| 10 | CS | High | 645 | 42.63 | 57.16 | 22.28 |
| 11 | **US** | **Low** | **745** | **30.71** | **41.05** | **25.79** |
| 12 | **CS** | **Low** | **745** | **31.01** | **41.39** | **25.69** |
| 13 | US | High | 845 | 45.23 | 60.59 | 22.76 |
| 14 | CS | High | 845 | 41.55 | 55.73 | 23.86 |
| 15 | **US** | **Low** | **945** | **30.33** | **40.57** | **27.28** |
| 16 | **CS** | **Low** | **945** | **31.78** | **42.42** | **26.69** |
| 17 | US | Median | 1045 | 36.28 | 48.84 | 25.76 |
| 18 | CS | Median | 1045 | 34.32 | 46.27 | 26.47 |

significance level, respectively. If the calculated $t$ value for a paired scenario generated by Models US and CS is greater than the right critical $t$ value, Model CS is better than Model US based on the average delay in the network. If such a $t$ value is less than the left critical $t$ value, Model CS is better than Model US based on the average speed in the network.

Figure 5 depicts the results of Student's $t$-tests for the average delay and speed in the network under different levels of traffic demands at 1% significance level. Herein, the average delay and speed in the network are defined as the average values of the delays and speeds for all the vehicles from origins to destinations in the network, respectively. It can been found that Model CS performs better than Model US under the median and high levels of traffic demands at 1% significance level, whereas the difference between both of them is not significant under the low level of traffic demands at the same significance level. This viewpoint is also proven by the data listed in Table 5. Each given data point is the mean of the sample values from the multirun simulation.

The correlation analysis is carried out to analyze the aggregated data in Table 5. Herein the average delay at paired intersections is defined as the average value of the delays for all the vehicles from starting to ending sections at either of paired intersections, and it is aggregated using the delay data measured by the travel time sections. Also, the average delay in the network is aggregated using the delay data measured by the network performance evaluation. The findings show that the average delay at paired intersections is strongly and positively related to the average delay in the network, and these two average delays are both negatively related to the average speed in the network at the medium level.

## 5. Discussion and Suggestions

As stated before, the effective green times and the left-turn bay lengths obtained by adopting Models US and CS strongly depend on traffic demands, and they have nothing to do with intersection spacing. However, the offset between paired intersections obtained by utilizing Model CS is very sensitive to intersection spacing. The performance of each formulated model relies on all the decision variables. Moreover, some model parameters may have significant effects on the optimized values of these decision variables.

Regarding equations (13) and (18), the initial queue may affect the optimized values of the effective green times and the left-turn bay lengths. If the formulated models are applied for future design, the initial queue can be set to 0, as mentioned above. If they are applied in reality, the initial queue should be calibrated by observation.

Regarding equation (18), the number of vehicles in a platoon has an important influence on the optimized value of the offset between paired intersections. When the intersection spacing is certain, such an offset is very sensitive to the number of vehicles in a platoon [32]. If Model CS is used for future design, the number of vehicles in a platoon can be set to 20 pcu, as shown earlier. If this model is used in reality, such a parameter should also be calibrated by observations.

Due to arbitrary driving behaviors, traffic flow stochastically fluctuates with time. Thus, it is very hard and laborious to acquire the accurate initial queue and number of vehicles in a platoon, and it is unnecessary to do this. The suggestions are as follows: the first step is to obtain the optimal combination of signal timings and left-turn bay lengths using the formulated models and the recommended parameters; the second step is to adjust the offset between paired intersections on the basis of the ascertained effective green times and left-turn bay lengths if Model CS being adopted and necessary [22].

Based on the aforementioned numerical and simulation experiments, Model CS usually performs better than Model

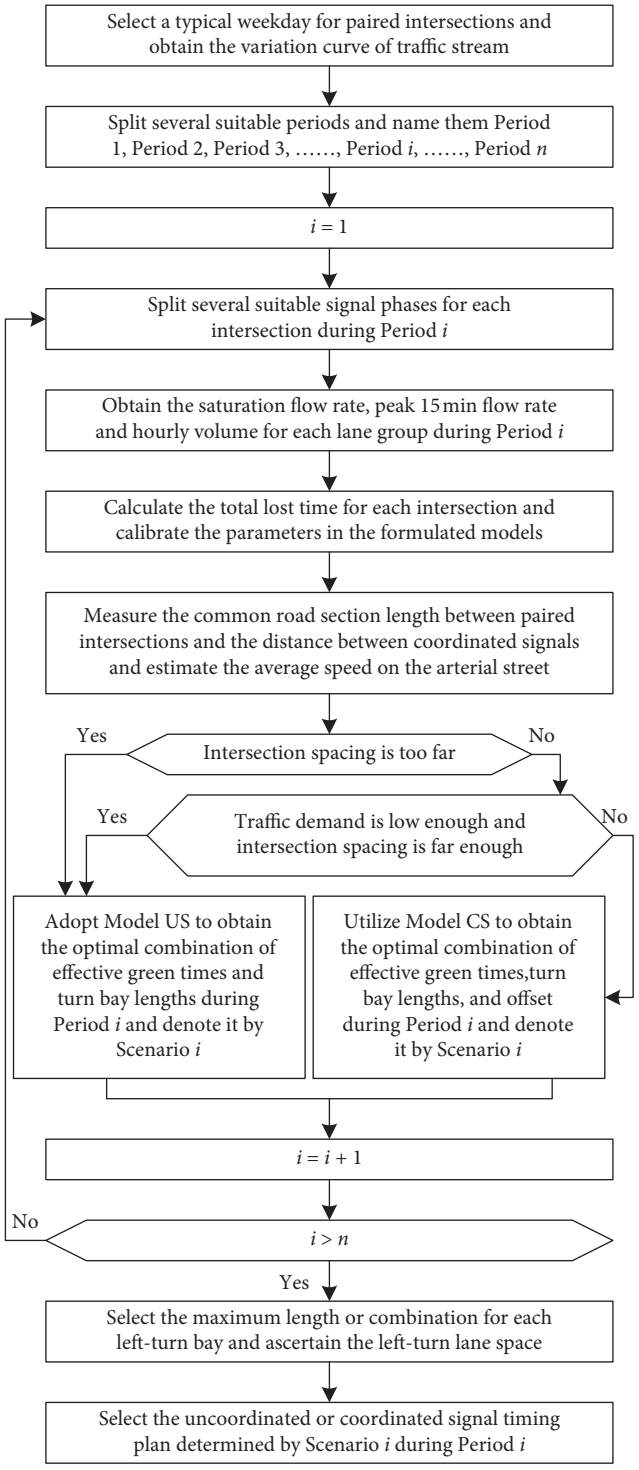


Figure 6: Flowchart of model application.

US when traffic demand is high enough, whereas the former may be worse than the latter when traffic demand is low enough and intersection spacing is far enough.

The aforementioned analysis is to discuss the optimal combination of signal timings and left-turn bay lengths on a peak period basis. Actually, signal timings often vary from one period to another period, whereas left-turn bay lengths generally remain unchanged during all the periods in several months or years. Considering the fluctuation of traffic stream and the stability of turn bay space, the application of the formulated models is proposed, as illustrated in Figure 6. If the relevance of traffic flow exists, Model US is used when the distance between paired intersections is too far, or such a distance is far enough, and traffic demand is low enough; otherwise, Model CS is utilized.

## 6. Conclusions

At signalized intersections, left-turn bays have an important effect on intersection operations. Focusing on a pair of intersections with left-turn bays, such an effect should also be considered. If these two intersections are closely spaced and the relevance of traffic stream exists, coordinated signals will have to be concerned. The expressions of the capacity and delay are first specified together with the basic assumptions and some constraints. Next, two single-objective optimization models are presented for paired intersections with uncoordinated and coordinated signals. Then, some numerical examples are given to demonstrate the application of these two models. The outcomes indicate the following: the optimized values of the effective green times and the left-turn bay lengths obtained by utilizing the proposed models depend on traffic demand and are not sensitive to intersection spacing; intersection spacing has a significant effect on the optimized value of the offset between paired intersections obtained by adopting the model with coordinated signals; and the performance of the optimization model with coordinated signals is better than that with uncoordinated signals at 99% confidence level.

To testify the performance of the proposed models, the orthogonal simulation experiments are designed and fulfilled using the *VISSIM* software. The findings reveal the following: the optimization model with coordinated signals performs better than that with uncoordinated signals at 99% confidence level when traffic demand is high enough and the distance between paired intersections is near enough, whereas the former does not always outstrip the latter when traffic demand is lower than a threshold and intersection spacing is greater than a threshold. Some discussion and suggestions are also explained.

The contributions of this article are as follows: (1) concerning paired intersections with left-turn bays, one single-objective optimization model with uncoordinated signals is reformulated and compared with the optimization model with coordinated signals, and these two models can be applied to the cases without left-turn bays; (2) the flowchart of using the formulated models in practice is put forward under various conditions.

In the future research, the field data and other traffic simulation software packages will be utilized to further investigate the effectiveness and reliability of the formulated models. Furthermore, these two models need to be improved so that they can be used on an arterial street, in a regional traffic network or for mixed traffic.

## Data Availability

The data used to support the findings of this study are available from the corresponding author upon request.

## Conflicts of Interest

The authors declare that they have no conflicts of interest.

## Acknowledgments

This research was supported by the National Natural Science Foundation of China under Grant no. 51578111.

## References

[1] Transportation Research Board (TRB), *Highway Capacity Manual 2010 (HCM 2010)*, National Research Council, Washington, DC, USA, 5th edition, 2010.

[2] C. J. Messer and D. B. Fambro, "Effects of signal phasing and length of left-turn bay on capacity," *Transportation Research Record*, vol. 644, pp. 95–101, 1977.

[3] R. Akçelik, *Traffic Signals: Capacity and Timing Analysis*, Australian Road Research Board (ARRB) Transport Research Ltd., Victoria, Australia, 1981.

[4] J. J. Lee, N. M. Rouphail, and J. E. Hummer, "Models for lane utilization prediction for lane drop intersections," *Transportation Research Record*, vol. 1912, pp. 47–56, 2005.

[5] T. Sando and R. Moses, "Influence of intersection geometrics on the operation of triple left-turn lanes," *Journal of Transportation Engineering*, vol. 135, no. 5, pp. 253–259, 2009.

[6] Z. Z. Tian and N. Wu, "Probabilistic model for signalized intersection capacity with a short right-turn lane," *Journal of Transportation Engineering*, vol. 132, no. 3, pp. 205–212, 2006.

[7] N. Wu, "Total approach capacity at signalized intersections with shared and short lanes: generalized model based on a simulation study," *Transportation Research Record*, vol. 2027, pp. 19–26, 2007.

[8] Y. Zhang and J. Tong, "Modeling left-turn blockage and capacity at signalized intersection with short left-turn bay," *Transportation Research Record*, vol. 2071, pp. 71–76, 2008.

[9] A. Osei-Asamoah, A. Kulshrestha, S. S. Washburn et al., "Impact of left-turn spillover on through movement discharge at signalized intersections," *Transportation Research Record*, vol. 2173, pp. 80–88, 2010.

[10] K. Yin, Y. Zhang, and B. X. Wang, "Modeling delay during heavy traffic for signalized intersections with short left-turn bays," *Transportation Research Record: Journal of the Transportation Research Board*, vol. 2257, no. 1, pp. 103–110, 2011.

[11] Z. Li and L. Elefteriadou, "Maximizing the traffic throughput of turn bays at a signalized intersection approach," *Journal of Transportation Engineering*, vol. 139, no. 5, pp. 425–432, 2013.

[12] S. Kikuchi, P. Chakroborty, and K. Vukadinovic, "Lengths of left-turn lanes at signalized intersections," *Transportation Research Record*, vol. 1385, pp. 162–171, 1993.

[13] S. Kikuchi, M. Kii, and P. Chakroborty, "Lengths of double or dual left-turn lanes," *Transportation Research Record*, vol. 1881, pp. 72–78, 2004.

[14] S. Kikuchi, N. Kronprasert, and M. Kii, "Lengths of turn lanes on intersection approaches," *Transportation Research Record: Journal of the Transportation Research Board*, vol. 2023, no. 1, pp. 92–101, 2007.

[15] S. Kikuchi and N. Kronprasert, "Determining lengths of left-turn lanes at signalized intersections under different left-turn signal schemes," *Transportation Research Record*, vol. 2195, pp. 70–81, 2010.

[16] Y. G. Qi, L. Guo, L. Yu, and H. Teng, "Estimation of design lengths of left-turn lanes," *Journal of Transportation Engineering*, vol. 138, no. 3, pp. 274–283, 2012.

[17] J. Yang and H. Zhou, "Integrating left-turn lane geometric design with signal timing," *Journal of Transportation Engineering*, vol. 137, no. 11, pp. 767–774, 2011.

[18] R. Yao and H. Michael Zhang, "Optimal allocation of lane space and green splits of isolated signalized intersections with short left-turn lanes," *Journal of Transportation Engineering*, vol. 139, no. 7, pp. 667–677, 2013.

[19] R. H. Yao, "Settings of short left-turn lane and signal phase sequence for isolated signalized intersections," *Transport*, vol. 31, no. 4, pp. 416–426, 2016.

[20] R. H. Yao, H. M. Zhou, and Y. E. Ge, "Optimizing signal phase plan, green splits and lane length for isolated signalized intersections," *Transport*, vol. 33, no. 2, pp. 520–535, 2018.

[21] R. Yao, "Sensitivity analysis of optimization models for two adjacent intersections with correlated short left-turn lanes," *Transport*, vol. 28, no. 3, pp. 256–269, 2013.

[22] R. Yao, W. Guo, and H. Zhou, "Integrative design of left-turn lane space and signal coordination for two adjacent intersections," *Canadian Journal of Civil Engineering*, vol. 44, no. 4, pp. 274–285, 2017.

[23] N. H. Gartner, S. F. Assman, F. Lasaga, and D. L. Hou, "A multi-band approach to arterial traffic signal optimization," *Transportation Research Part B: Methodological*, vol. 25, no. 1, pp. 55–74, 1991.

[24] C. Zhang, Y. Xie, N. H. Gartner, C. Stamatiadis, and T. Arsava, "AM-Band: an asymmetrical multi-band model for arterial traffic signal coordination," *Transportation Research Part C: Emerging Technologies*, vol. 58, pp. 515–531, 2015.

[25] H. Hou and H. X. Liu, "Arterial offset optimization using archived high-resolution traffic signal data," *Transportation Research Part C: Emerging Technologies*, vol. 37, pp. 131–144, 2013.

[26] Y. Y. Chen and G. L. Chang, "A macroscopic signal optimization model for arterials under heavy mixed traffic flows," *IEEE Transactions on Intelligent Transportation Systems*, vol. 15, no. 2, pp. 805–817, 2014.

[27] Road and Transportation Research Association (RTRA), *Guidelines for Traffic Signals (RiLSA)*, Steering Committee for Traffic Control and Traffic Safety, Cologne, Germany, 2003.

[28] R. P. Roess, E. S. Prassas, and W. R. McShane, *Traffic Engineering*, China Machine Press, Beijing, China, 3rd edition, 2008.

[29] K. Lu and J. Xu, "Offset model for arterial road coordinate control and its optimization method," *China Journal of Highway and Transport*, vol. 21, no. 1, pp. 83–88, 2008.

[30] R. H. Yao, *A Study on Vehicular Queue Models*, Doctoral Dissertation, Jilin University, Changchun, China, 2007.

[31] J. Sun, *Guideline for Microscopic Traffic Simulation Analysis*, Tongji University Press, Shanghai, China, 2014.

[32] R. Yao, X. Zhang, N. Wu, and X. Song, "Modeling and control of variable approach lanes on an arterial road: a case study of Dalian," *Canadian Journal of Civil Engineering*, vol. 45, no. 11, pp. 986–1003, 2018a.